The structure and dynamics of dense nitrogen gas. II

1993 J. Phys.: Condens. Matter 5 4265

(http://iopscience.iop.org/0953-8984/5/26/001)

J. Phys.: Condens. Matter 5 (1993) 4265–4270. Printed in the UK

The structure and dynamics of dense nitrogen gas: II

P Backx†§, P A Lonngi‡ and P A Egelstaff†

† Department of Physics, University of Guelph, Canada

‡ Universidad Autonoma Metropolitana–Iztapalapa, Mexico

Received 22 January 1993, in final form 31 March 1993

Abstract. Neutron scattering measurements of the dynamic structure factor for dense nitrogen gas have been reported in a previous paper. We carried out computer simulations of dense nitrogen gas at room temperature, for densities between 7.1 and 12.1 molecules nm^{-3}, to obtain a prediction for the dynamic structure factor. Compared to the previous experimental results the simulation data showed generally good agreement except for in the ranges ($Q < 1$ Å^{-1}; $\omega < 3$ ps^{-1}) and ($Q > 2$ Å^{-1}; $\omega > 10$ ps^{-1}), where the simulated data fell below the experimental data. These observations probably indicate deficiencies in the intermolecular potential employed in the simulation over longer ranges (~ 10 Å), and also for fast impacts ($< 10^{-13}$ s).

1. Introduction

In a previous paper [1], we discussed a measurement via neutron inelastic scattering of the dynamic structure factor of dense nitrogen gas at several states along the room temperature isotherm. Results for the *static* structure factor, obtained by integrating the experimental results, were presented and compared to a computer simulation based on a published model intermolecular potential [2]. This model involved an isotropic site–site Lennard-Jones interaction and long-range quadrupole–quadrupole terms. The agreement was good in general, and we concluded that a simulation of the full dynamic structure factor using the same potential would be justified. Thus we have carried out this simulation, and here we describe its comparison to the previous experimental results. This comparison may be expected to be a more severe test of the model potential, and in particular tests long- and short-range effects separately. For example it will test the performance of the model potential in predicting the dynamics of fast impacts at times $< 10^{-13}$ seconds. However, improvements to the model potential would require *ad hoc* changes, and further simulations.

In section 2 we describe the simulation method and results, in section 3 the handling of the experimental data (of figure 1 for example), and in section 4 we present their comparison. The data extend from 0.5 to 4 Å^{-1}, that is over the region of the principal peak in the static structure factor.

2. Computer simulation of $S(Q, \omega)$

The simulation of the static structure factor was discussed in our earlier work [1], and we used the same procedure here except that the number of molecules was doubled to 500 (i.e.

§ Present address: Faculty of Medicine, Johns Hopkins University, Baltimore, MD, USA.

0953-8984/93/264265+06$07.50

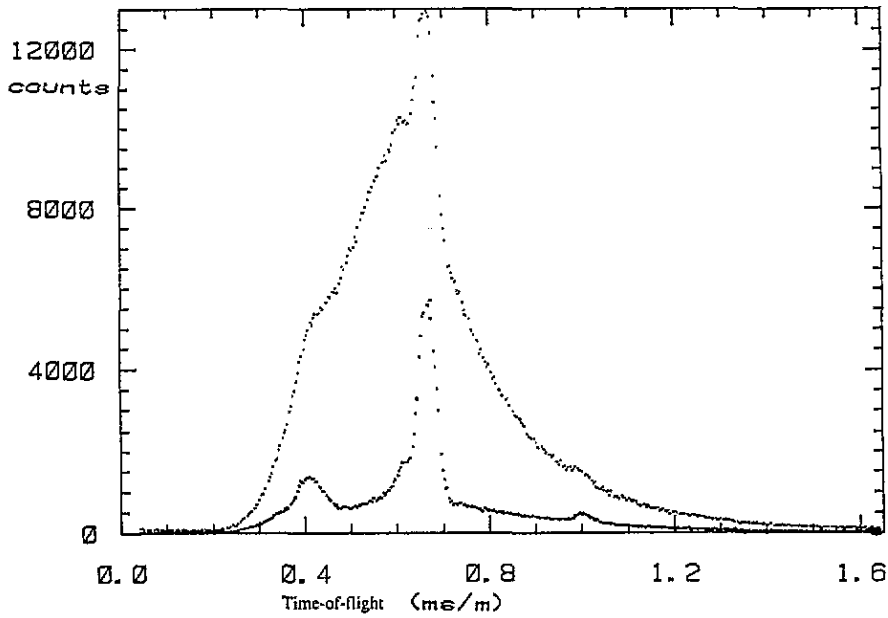

Figure 1. Scattered neutron intensity as a function of time of flight for an angle of 76.5° and a density of 10.6 molecules nm^{-3}. The upper set of points is the pressure vessel plus nitrogen and the lower set of points is for the pressure vessel alone. On this scale the FWHM of the resolution function was 0.0125 ms.

1000 atoms). Four states at densities of 12.1, 10.6, 8.76 and 7.13 molecules nm^{-3} were simulated using the site–site plus quadrupoles model potential of Cheung and Powles [2] in a program provided by Haile [3]. Initially the particles were placed on an FCC lattice with velocities assigned randomly and scaled to give a temperature of 296 K. The system was equilibrated for 2000 time steps, and we noted that melting of the lattice occurred after 500–700 time steps (of 0.5034×10^{-14} s). The temperature was rescaled periodically: the system was followed for 8000 time steps and the positions of all nitrogen atoms were stored every five time steps. During this procedure the temperature remained constant to within one part in 500.

The dynamic structure factor, $S(Q, \omega)$, is related to an intermediate scattering function, $I(Q, t)$, by the equation

$$S(Q, \omega) = \frac{1}{2\pi} \int_{-\infty}^{+\infty} I(Q, t) \exp(-i\omega t)\, dt \tag{1}$$

where $\hbar Q$ and $\hbar\omega$ are the momentum and energy transferred in the scattering process. It is important to check the numerical quality of the simulation data and therefore the function $I(Q, t)$, was evaluated in two ways to provide an initial test of the data:

$$I(Q, t) = \frac{1}{N} \left\langle \sum_{ij} \exp(\mathrm{i} Q r_{ij}) \right\rangle \tag{2a}$$

or

$$I(Q, t) = \frac{1}{N} \left\langle \sum_{ij} \frac{\sin Q r_{ij}(t)}{Q r_{ij}(t)} \right\rangle \tag{2b}$$

where $r_{ij}(t) = r_i(t) - r_j(0)$ and i or j denotes any atom (including $i = j$). It was found that there was agreement between (a) and (b) to one part in 1000, and subsequently only equation 2(b) was used. This function was evaluated for all $|r_{ij}| < 3.26$, the usual forward scattering term (e.g. [2]) was subtracted, and the evaluation was extended to 500 time steps at 100 equispaced points. The procedure was repeated for origins separated by 15 time steps throughout the data, and averaged to obtain the final $I(Q, t)$. In order to smooth the function $I(Q, t)$ at large t, we fitted the data above about 1 ps to an exponential function which gave a good fit.

Since the previous data [1] had not been corrected for the instrumental resolution function, the experimental dynamic structure factor was calculated from

$$S_E(Q, \omega) = \frac{1}{\pi} \int_0^\infty \cos \omega t \exp(-t^2/6.6)\ I(Q, t)\, dt. \tag{3}$$

In this equation t is in picoseconds, and the factor $\exp(-t^2/6.6)$ has been included [1] to allow for the instrumental resolution. Thus the function $S_E(Q, \omega)$ may be compared directly to the experimental results. Finally to obtain results at the densities listed in table 1 of [1], we interpolated between the four simulation densities using a least squares fit to a second-order equation. These data are plotted as squares in figures 2 and 3.

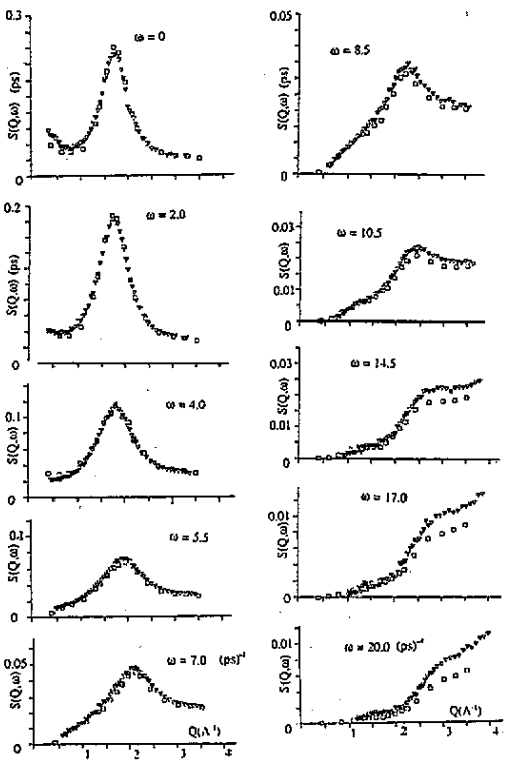

Figure 2. A comparison between the computer simulation (squares) and the experimental results (triangles) for nitrogen gas at a density of 12.1 molecules nm^{-3} and a temperature of 297 K. The quantity shown is $S_E(Q, \omega)$ of equation (3), plotted as a function of Q for fixed ω.

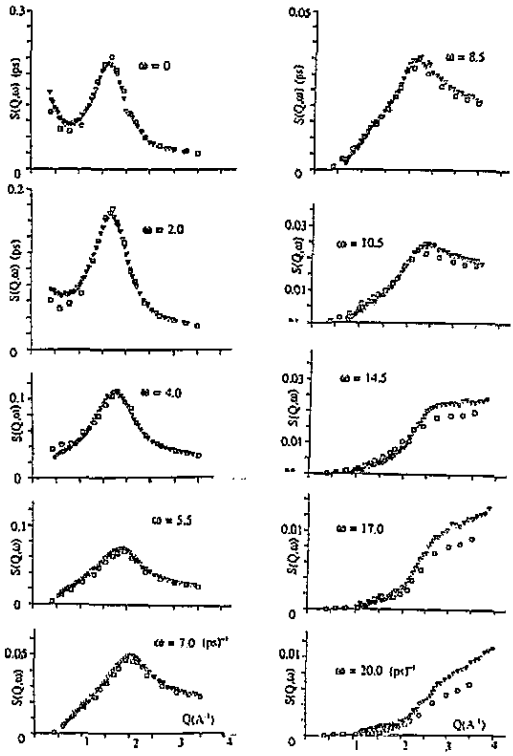

Figure 3. Same as figure 2 for a density of 9.61 molecules nm^{-3} and a temperature of 297 K.

3. Experimental data

The experiment was carried out on the IN4 apparatus at the ILL reactor (Grenoble), using an incident neutron energy of about 12 meV and conditions under which the FWHM of the resolution function was 1.2 meV. A pressure vessel, consisting of five parallel cylindrical holes of internal diameter 14.31 mm cut into an aluminium alloy block of 21.56 mm thickness, was used for collecting data at densities between 7.13 and 9.46 molecules nm^{-3}. A similar vessel, with holes of 6.50 mm diameter cut into a block of thickness 12.57 mm, was used for collecting data at densities between 8.76 and 12.10 molecules nm^{-3}. All measurements were carried out at room temperature, and the vessel temperature was measured for each run: the range of temperatures was 295.2 to 296.8 K, with exact values for each density being listed in table 1 of [1]. Other experimental parameters are given in table 2 of [1]. Figure 1 shows an example of the raw time-of-flight data for a run at a density of 10.6 molecules nm^{-3} (run b of table 1, [1]) at an angle of 76.5°. This demonstrates the statistical quality of the data and the relative contribution of the pressure vessel in the observed data. It shows also the range of variables over which good quality data may be extracted.

After subtraction of backgrounds and container scattering, the intensity as a function of angle was normalized by vanadium calibration. Then we observed that the intensity in the wings of the spectra was almost independent of angle, and therefore the spectra at the three lowest angles were used to fit an analytical model for the shape of the multiple scattering

(see Hawkins and Egelstaff [4]). After removing the usual detailed balance factor (e.g. [4]) to obtain an almost classical experimental result, the function $S_E(Q, \omega)$ was derived for each of sixty-two angles extending from 8.3° to 83.3°. As a check we integrated these results over ω, and were able to confirm our previous conclusions regarding the static structure discussed in [1].

The experimental points for $S_E(Q, \omega)$ were averaged in groups of four, to give a table of data at given ω (corresponding to the time-of-flight channels) and as a function of Q (corresponding to the sequence of angles). Finally we interpolated these data to find the specific values of ω required for the comparisons with the simulations. The resulting data are shown as triangles in figures 2 and 3. From the discussion above and in [1] it is evident that the most important errors will be residual systematic errors, which are difficult to estimate accurately. Nevertheless the data reduction and calibration procedures were reviewed, and we concluded that this residual uncertainty may account for 50% of the differences between the experiment and simulation seen at high ω in these figures.

4. Comparison between simulation and experiment

In figures 2 and 3 we show a comparison of the simulated and experimental results for a number of chosen values of ω. Overall the agreement is good, as might be expected from the previous comparison with the static structure. The agreement in the region of the peak is excellent and here an empirical interpretation of some effects is possible. For example, it may be shown from the theory of neutron scattering by polycrystalline samples (e.g. Lovesey [5]) that, when the polycrystalline $S(Q, \omega)$ is plotted in the form shown at figures 2 and 3, there will be a peak at Q values close to the Bragg condition and the peak Q values will (initially) be a linear function of ω. The slope of this linear function will be given by the appropriate velocity of sound. This behaviour is likely to be followed approximately in all dense samples, and therefore it is interesting to discover whether, at the gas densities used here, it is still observable. In figure 4 we plot the peak positions observed in figures 2 and 3. It may be seen that after remaining nearly constant (roughly over 0.25 $Å^{-1}$, or the half width at half maximum of the $\omega = 0$ peak), a linear slope develops which is close to that calculated from the velocity of sound at 12.1 molecules nm^{-3}. This observation thus confirms the generality of this empirical effect in inelastic spectra, at a semi-quantitative level.

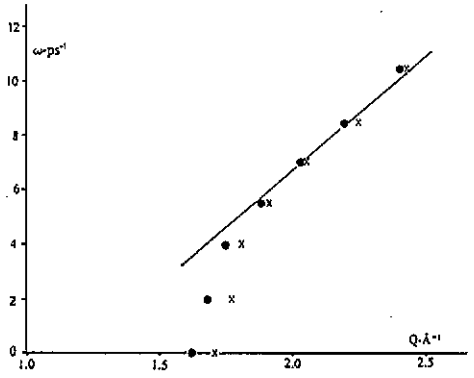

Figure 4. A plot of the peak positions determined from the data shown in figures 2 and 3, for $\omega \leqslant 10.5$ ps^{-1}. The line has been drawn with a slope corresponding to the velocity of sound (840 m s^{-1}) at the higher density (12.1 molecules nm^{-3}), and the circles and crosses are the data at 9.61 and 12.1 molecules nm^{-3} respectively.

However, the dynamic structure factor contains more detailed information than the static structure factor and some clear discrepancies are evident away from the peak intensity. For

$Q < 1$ Å^{-1} it is evident that the simulated data fall below the experimental data when $\omega < 3$ ps^{-1}. When coupled with the good agreement at higher Q, for $\omega < 10$ ps^{-1} this indicates that the potential describes the shorter-ranged features of intermolecular collisions but fails to describe the longer-ranged effects (5–15 Å) adequately. Over this range some modification is needed which will effectively slow down the dynamic behaviour.

In the range $5 < \omega < 8$ ps^{-1} there appears to be good agreement at all Q, while for $\omega > 10$ ps^{-1} the shapes of the curves are similar but the simulation has a somewhat lower magnitude. This may mean that the potential should be modified to increase high-frequency processes, but since the observed intensity here is about one-tenth of the intensity at $\omega = 0$ the systematic errors may account for some of this effect (see section 3). We note however that such modifications would need to be tested through the comparison of further MD simulations with the experimental data. In effect an iterative procedure is needed in which the short-ranged part of the potential is modified until a fit to data, such as that in figures 2 and 3, is achieved.

5. Conclusions

We have confirmed our previous conclusion that for nitrogen at room temperature, the intermolecular potential of Cheung and Powles [2] gives a good description of the static structure factor for dense nitrogen gas, and have extended this conclusion to the overall behaviour of the dynamic structure factor. However, because the dynamic structure factor is a more detailed function, a more detailed observation of the differences revealed by this comparison may be made. In particular the selectivity of this function should be useful, and may be demonstrated. For momentum transfers of less than 1 Å^{-1} and frequencies less than 3 ps^{-1} the intensity given by the model is less than observed, and therefore such neutron experiments are worth extending to lower Fourier components as they may be the most sensitive test of this model (or others) over this range. In addition a discrepancy is observed for ($Q > 2.5$ Å^{-1}; $\omega > 10$ ps^{-1}) which may be reviewed by methods similar to those employed by Boon and Yip [6] in a discussion of the sensitivity of parts of the velocity correlation function to features of the intermolecular potential or used for the same purpose by Rodger [7]. These experimental results indicate the need for improvements in the potential at short range, and might perhaps be interpreted further using perturbation theory (e.g. Egelstaff *et al* [8]). However, the magnitude is small, and firm conclusions should await improved experiments and further simulations.

References

[1] Egelstaff P A, Hawkins R K, Litchinsky D, Lonngi P A and Suck J-B 1984 *Mol. Phys.* **53** 389
[2] Cheung P and Powles J G 1976 *Mol. Phys.* **32** 1383
[3] Haile J M 1982 private communication; 1992 *Molecular Dynamics Simulation* (New York: Wiley)
[4] Hawkins R K and Egelstaff P A 1975 *Mol. Phys.* **29** 1639
[5] Lovesey S W 1984 *Theory of Neutron Scattering from Condensed Matter* (Oxford: Clarendon)
[6] Boon J P and Yip S 1980 *Molecular Hydrodynamics* (New York: McGraw-Hill) p 118
[7] Rodger P M 1992 *Mol. Phys.* **76** 1385
[8] Egelstaff P A, Gray C G, Gubbins K E and Mo K C 1975 *J. Stat. Phys.* **4** 315